THE PHYSICS OF SPIN INJECTION INTO DNA

BY XUE-FENG WANG AND TAPASH CHAKRABORTY

For many decades, the development of the traditional semiconductor-based devices has followed the Moore's law where it was predicted that the number of components per integrated circuit would double every 18 months as a result of the shrinking size of the components [1]. Up until 2006, the core wire width of the Intel CPU has become as thin as 65 nm and it is very possible that in one or two decades the structure of many key electronic devices will be in the nanoscale. On the other hand, the physical principle tells us that the quantum coherence effects on the electronic behavior become dominant in the nanoscale when the size of the electronic structures is comparable to the wavelength of the electrons inside. As a result, the quantum transport theory will rule the behavior of the electrons – the carriers of the information within the devices, as the traditional diffusion-drift electronic transport model will fail. Quantum computation is expected to be the principle in future computers. There are additional concerns about the production of these devices when they reach the nanoscale. For example, the lithographic techniques used in manufacturing present semiconductor device architecture is limited by the wavelength of the particles (photons or electrons) employed in these techniques. This means that the traditional "top-down" production process will reach its limits soon and alternative methods are now in great demand.

Based on the above concerns, researchers have begun to look for alternatives to the traditional semiconductors for future quantum computation. The qualifying materials should have some basic characteristics necessary for building a quantum computation system. At first, we need a reliable way to build small devices. One of the promising approach is the so called "bottom-up" method. In this picture, a device is built atom by atom or molecule by molecule. This can be done by picking atoms and putting them in the proper position. Another way is to make use of some special chemical properties of the molecules such as the self-assembling property of DNA. In this way, DNA has been considered as one of the promising candidates for molecular electronics [2,3]. As we all know, DNA is the molecule responsible for the storage of genetic information in the cells. Naturally, it is reliable in self-assembling and a DNA with defined sequences can be produced synthetically in the laboratory with the present techniques.

SUMMARY

DNA would play an important role in molecular electronics due to its self-assembly property. Spintronics in DNA may lead to nanoscale quantum computation.

Secondly, the system needs the quantum bit (Qubit) which represents the 0 and 1 in a computer. Promising candidates for this purpose include the photon polarizations, energy levels in quantum dots or in atoms, and the two spin polarizations of spin-½ particles like electrons or neutrons. In this respect, the two spin states (spin-up or spin-down) of electrons have been regarded as a very natural choice. Based on this expectation, spintronics has been one of the most attractive topics in the last decade [4,6] and spintronics in DNA is also becoming very appealing [7,8].

To realize the spin transport in DNA, it is very important to be able to manipulate the transport of electrons, the carriers of spin, in the molecular level. In the past decades, a remarkable progress in direct measurements of the electron transport through DNA has made this operation very attractive [2,3,7,9-13], although the full control of the electronic transport in DNA seems still difficult. In this article, we address some primary aspects of the spintronics in DNA using the Poly(G:C) chain as a prototype. To do so, a spin transport system is established by connecting the DNA chain into an electric circuit of constant voltage via a ferromagnetic electrode to the left as the spin injector and a ferromagnetic electrode to the right as the spin analyzer. When we switch the magnetization orientation of the spin analyzer from parallel to anti-parallel to that of the spin injector, the current I over the system varies if the electrons passing through the DNA are spin polarized, i.e., the spin is injected into the DNA. Consequently, we may observe a non-zero magnetoresistance defined as the percentage change of resistance R between the parallel and the anti-parallel configurations, $R_m = (R_{anti} - R_{paral}) / R_{anti} = (I_{paral} - I_{anti}) / I_{paral}$. The numerical simulation shows that the injection of spin into DNA is very likely. Furthermore, in the presence of the spin-orbit interaction, an enhancement and oscillations of the magnetoresistance are observed.

DNA consists of two-chain polymers of the nucleotide units – the DNA duplex. Each nucleotide contains three components: a heterocyclic base, a deoxyribose sugar, and a phosphate. The sugar and the phosphate of the successive nucleotide units along each chain are connected in an alternating sequence and form the backbone of the chain. The base of each nucleotide attaches to the sugar on one

Xue-Feng Wang, Atomistix Asia Pacific, Pte. Ltd., 50 Nanyang Drive, NTU Singapore 637 553.

Tapash Chakraborty <chakrabt@cc.umanitoba.ca>, Canada Research Chair Professor, Department of Physics and Astronomy, University of Manitoba, R3T 2N2

side and to its counterpart base from the other chain on the other side. The two chains are held together through pairing of their bases by hydrogen bonds. There are four kinds of bases, two purine derivatives, guanine (G) and adenine (A), and two pyrimidine derivatives, cytosine (C) and thymine (T). The pairing occurs only between the G and C by three hydrogen bonds or between the A and T by two hydrogen bonds, i.e. there are only two kinds of Watson-Crick base pairs, (G:C) and (A:T). The distance between the neighboring base pairs is about 0.34 nm. Usually, the charge transport in DNA occurs via electronic transitions among the highest occupied molecular states (HOMO) (*p*-type hole transport) or among the lowest unoccupied molecular states (LUMO) (*n*-type electron transport) of the bases [14]. Based on the existing experiments and the *ab initio* results, it has been suggested that the energy gap between the HOMO and LUMO states in each base is about 4 eV [3] and the charge transport in DNA is mainly *p*-type, such as the case for the short 30-basepair Poly(G:C) DNA duplex used in Ref. [9].

Microscopic and macroscopic models have been established to quantitatively calculate the charge transport in DNA. In the former case the system is handled via the first principle; the outer-shell orbits of all atoms in the system and the coupling between them are taken into account explicitly and the transport properties of the system are obtained by the *ab initio* calculations. For the macroscopic models, crucial physical information is extracted from the *ab initio* calculations and are parameterized to simplify the system in the hope of being able to handle bigger systems and also obtain more physical insights than those available from the *ab initio* calculations. Here we shall discuss the spin transport based on a macroscopic tight-binding model. In this model, the system is composed of a series of sites where each site corresponds to a HOMO state of a base and is described by the on-site energies for the HOMO energies of the bases and the coupling parameters between the sites for coupling of the HOMO states between the bases.

The on-site energy of each base is the energy to create a hole in the HOMO state of the base, viz., the ionization energy. The ionization energy is sensitive to the existence of other bases around and also to the environment. This value for the single bases can be calculated by the quantum chemical *ab initio* methods and were confirmed by measurements in the bases' gas phase. The calculated HOMO hole energies for the isolated single bases G, C, T, and A are $E_G = 7.75$, $E_C = 8.87$, $E_T = 9.14$, and $E_A = 8.24$ eV respectively [12,15,16]. It is to be noted that these values may depend on the method used [17]. Just as for the on-site energies of the bases, the coupling parameters between different sites (bases) in principle can also be calculated by the *ab initio* methods. Usually, this effective coupling parameter depends on how the macroscopic model is established. While the intrinsic value comes from the overlap of the HOMO wave functions between the bases, the effective one should be adjusted if other factors, such as the environment and the phonon, are not explicitly taken into account in the model. Until now, the calculated coupling parameter from different *ab initio* models are scattered in a range of 0.01 - 0.4 eV [15,18]. Nevertheless, some common qualitative characteristics of the coupling have been extracted from these calculations. Although the purine and pyrimidine bases within each Watson-Crick base pair are strongly coupled by the hydrogen bonds, the hydrogen bonds do not participate in the carrier transport because they have a lower energy than the HOMO states. As a result, the interstrand coupling parameter for the HOMO states between them is much weaker than the intrastrand coupling parameter between the neighboring bases along the DNA strands [18]. The coupling parameters are also sensitive to the relative position of the two bases in question and a twist of the DNA duplex may modify the coupling parameters significantly [3].

In a short Poly(G:C) DNA duplex, the electron transport occurs mainly via the pyrimidine Poly(G) chain because the base G has a much lower HOMO energy than that of the base C. Consequently, we can simply treat the DNA duplex as a chain of Poly(G). The Hamiltonian of the system reads

$$H = \sum_{\sigma} \sum_{n=-\infty}^{\infty} [\bar{\varepsilon}_n^{\sigma} c_{n,\sigma}^{\dagger} c_{n,\sigma} - t_{n,n+1}^{\sigma} (c_{n,\sigma}^{\dagger} c_{n+1,\sigma} + c.c.)] - \sum_{\sigma} \sum_{n=1}^{N-1} t_{n,n+1}^{s} (c_{n,\sigma}^{\dagger} c_{n+1,\bar{\sigma}} + c.c.).$$

Here $c_{n,\sigma}^{\dagger}$ is the creation operator of the hole with spin $\sigma = -\bar{\sigma} = \pm$ on site n of the DNA chain (for $1 \le n \le N$), of the left electrode ($n \le 0$), and of the right electrode ($n \ge N + 1$).

The DNA chain is characterized by three parameters, the effective (dressed) on-site energy of holes $\bar{\varepsilon}_n^{\sigma} = \varepsilon_d + \Sigma_d$ ($1 \le n \le N$), the effective coupling parameter $t_{n,n+1}^{\sigma} = t_d$ ($1 \le n \le N$-1) between any two nearest neighbor sites, and the spin-orbit parameter $t_{n,n+1}^{s} = t_d^2$. Here ε_d indicates the HOMO energy of each G base and the complex self-energy Σ_d phenomenologically takes into account the effects of the backbone, the environment, and the phonon. Here Σ_d is obtained by modelling the environment as a semi-infinite dephasing chain [8]. Its real part represents an adjust to the on-site energy and its imaginary part describes the dephasing effect. The Fermi energy in the isolated *p*-type DNA is usually located close to and above the HOMO energy.

The two electrodes are described phenomenologically by two semi-infinite chains with spin (σ)-dependent on-site energies $\bar{\varepsilon}_n^{\sigma} = \varepsilon_{mX}^{\sigma}$ ($n \le 0$ or $n \ge N + 1$) equal to the center of the conduction band and a coupling parameter $t_{n,n+1}^{\sigma} = t_{mX}^{\sigma}$ ($n \le$ -1 or $n \ge N + 1$) equal to one fourth of the conduction band width. Here $X = L$ or R denote the left or right electrodes. For realistic metal electrodes, there are several energy bands involved in the charge/spin transport and the characteristic parameters $\varepsilon_{mX}^{\sigma}$ and t_{mX}^{σ} are the average values of all the energy bands. In the quasi-equilibrium situation, they can be estimated from the electronic properties near the Fermi surface. In the far from equilibrium case, when a large bias is applied over the system

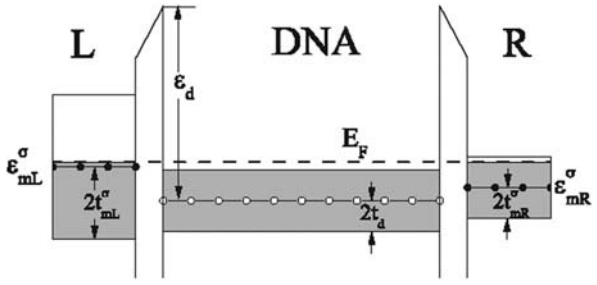

Fig. 1 **Schematic energy band** for holes of spin σ of the system in equilibrium when the on-site self energy and spin-flip effects are absent.

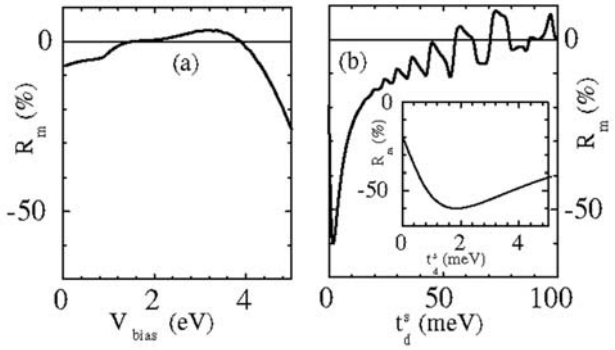

Fig. 2 **The magnetoresistance versus the bias voltage** in the absence of spin-orbit interaction (a) and versus the spin-orbit parameter t^s_d in DNA when a bias of 4.8 eV is applied (b).

as in the experiment of Ref. [9], these parameters are energy dependent for a realistic conduction band. In the following, we assume that the parameters of the one-dimensional tight-binding model have a similar dependence on the energy as in bulk materials and the dependence is extracted from the three-dimensional band structure of the materials. The parameters are then scaled to match the known values at the Fermi energy. Ferromagnetic Fe which exemplifies the electrode material here, has approximately five bands near the Fermi energy of the bulk material [21]. For the spin-up (majority) holes, the five bands are located approximately at 2.5, 0, -0.68, -3.4, and -7 eV above the Fermi energy with band width 6, 0.3, 0.6, 4.1, and 3.7 eV respectively. For the spin-down (minority) holes, the energy bands are the same as above but shifted 2.58 eV to higher energy. Using the Lorentzian broadening, we can mimic the bulk DOS and extract the parameters $\varepsilon^{\sigma}_{mX}$ and t^{σ}_{mX} [8].

The contact property between the electrodes and the DNA duplex depends on the material of the electrode, the geometry of the contact, and the environment, and is by itself an active field of research in both physics and chemistry [19]. How a DNA duplex contacts to the charge source or the drain determines the efficiency of the charge and spin injection and affects the measured results in the experiments. Unfortunately, in many cases the details of the contact, especially between the metal and DNA in direct transport measurements are not very clear yet. In the tight-binding model, an effective contact parameter t_{dm} is used to phenomenologically describe the contact and is assumed to be spin independent. With the contact, tunnelling barriers form between the DNA chain and the electrodes and exchange of holes between them becomes possible. In equilibrium, as illustrated in Fig. 1, the Fermi energies of the electrodes and of the DNA match with each other. When a voltage drop is applied between the source and the drain [20], the contact may significantly modify the potential profile across the DNA and the on-site energies vary accordingly. In the experiment of Ref. [9], the contact is very weak and the voltage drop occurs mainly at the contacts.

Some parameters of the system are extracted from fitting the experimental data of Ref. [9] based on the known Platinum's band structure [22]. The effective hopping parameter is t_d = 0.6 eV; the equilibrium Fermi energy is 1.73 eV higher than the DNA HOMO on-site energy ε_d; and the 1/3 (2/3) of the bias voltage drops at the right (left) contact corresponds to a contact parameter of t_{dm} = 0.019 eV (0.013 eV). In the following, t_{dm} = 0.02 eV is used for the Fe-DNA contacts. Since this parameter is obtained from the Pt-DNA contacts, the following numerical result might describe the spin injection process from Fe electrodes only qualitatively.

In Fig. 2(a), the magneto-resistance versus the applied voltage is plotted at a zero spin-orbit interaction. One interesting observation here is the appearance of the negative magneto-resistance, i.e., the current is enhanced in the anti-parallel configuration as a result of the quantum coherence. Another interesting observation is the stronger spin injection at a bias potential difference comparable to the average energy bandwidth, a result of the energy band mismatch between the two electrodes. In Fig. 2(b), we present the dependence of the magneto-resistance on the spin-orbit interaction [6] in DNA when a bias of 4.8 eV is applied. The magneto-resistance does not decay monotonically to zero as the spin-orbit interaction increases. Instead, the magneto-resistance is enhanced when the spin-orbit interaction is weak (t^s_d < 1.9 meV) as a result of the quantum coherence in the system. In the transmission spectrum, the peaks are slightly split with an increase of t^s_d, indicating mixing of the spin-up and spin-down states in the system due to the spin-orbit interaction. We observe an increase in the magneto-resistance from 20% at t^s_d = 0 to 60% at t^s_d = 1.9 meV as illustrated in the inset of Fig. 2(b). The magneto-resistance decreases smoothly with t^s_d for 2 meV < t^s_d < 20 meV and oscillates for higher t^s_d when its average decays to zero.

The strong spin effect at a weak spin-orbit interaction observed in the numerical calculation originates from two features of the system: the weak contact coupling between the electrodes and the DNA chain and the coherence of the system. Since the coupling between the electrode and the DNA chain is much weaker (of the order of 10 meV) than the coupling between the

neighboring sites inside the electrodes and the DNA chain (of the order of eV), the quantum transport shows strong resonance to the energy spectrum of the DNA chain and the transmission peaks become very narrow (with a width of the order of 10 meV when the thermal effect and the dephasing effect are taken into account). The spin-orbit interaction split each of these peaks by a spread of the order of the interaction strength. Its effect on the magneto-resistance is strong when each of the transmission peaks is partially split and becomes weaker after fully split into two independent peaks. As a consequence, the magneto-resistance maximizes at t_d^s equal to several meV and decays as it goes to several tens of meV. Oscillations of the magnetic resistance are a result of the coherence and occur as the two spin peaks are well separated. In other words, this reflects the spin precession of the holes when they travel along the DNA chain. Similar phenomena were previously observed in other semiconductor systems with the Rashba spin-orbit interaction [5,6]. Different from the cases in semiconductor nanostructures, here the energy band is non-parabolic and carriers in a wider range of energies are involved. The precession effect is consequently averaged out at a weak spin-orbit interaction.

In summary, DNA should be able to play an important role in molecular electronics due to its self assembly property. Furthermore, quantum spin injection into DNA is very likely and spintronics in DNA may lead to a solution to the quantum computation. This determination is based on the simulation of the magneto-resistance over a short DNA chain connected to ferromagnetic electrodes. The tight-binding model is employed to describe the system with parameters determined from the experimental results and the realistic energy bands of metals. The numerical simulation shows that the spin transport can be sensitive to the energy band structure of the ferromagnetic electrodes. In the presence of the spin-orbit interaction in DNA, enhancement and oscillation of the magneto-resistance due to mixing of the spin states are also observed. These can be observed in a system similar to that in Ref. [9] but with the ferromagnetic electrodes.

ACKNOWLEDGEMENTS

The work has been supported by the Canada Research Chair Program and the Canadian Foundation for Innovation (CFI) Grant.

REFERENCES

1. G.E. Moore, *Electronics*, **38** (1965). See for example, ftp://download.intel.com/research/silicon/moorespaper.pdf.
2. E. Braun and K. Keren, *Adv. Phys*., **53**, 441 (2004); C. Dekker and M.A. Ratner, *Phys. World*, **14**, 29 (2001).
3. R.G. Endres, D.L. Cox, and R.R. Singh, *Rev. Mod. Phys*., **76**, 195 (2004).
4. D.D. Awschalom, D. Loss, and N. Samarth (Eds.), *Semiconductor Spintronics and Quantum Computation* (Springer, 2002); *Proceedings of the First International Conference on the Physics and Applications of Spin Related Phenomena in Semiconductors*, edited by H. Ohno [*Physica E* **10** (2001)].
5. C.-M. Hu and T. Matsuyama, *Phys. Rev. Lett*., **86**, 66803 (2001).
6. Y.A. Bychkov and E.I. Rashba, *J. Phys. C*, **17,** 6039 (1984); S. Datta and B. Das, *Appl. Phys. Lett*., **56**, 665 (1989); X.F. Wang, P. Vasilopoulos, and F.M. Peeters, *Phys. Rev. B*, **65,** 165217 (2002); P. Pietiläinen and T. Chakraborty, *ibid*., **73**, 155315 (2006).
7. M. Zwolak and M. Di Ventra, *Appl. Phys. Lett*., **81**, 925 (2002).
8. X.F. Wang and T. Chakraborty, *Phys. Rev. B*, **74**, 193103 (2006).
9. D. Porath, A. Bezryadin, S. de Vries, and C. Dekker, *Nature*, **403**, 635 (2000).
10. X.Q. Li and Y.J. Yan, *Appl. Phys. Lett*., **79**, 2190 (2001).
11. P. Carpena, P. Bernaola-Galvan, P.C. Ivanov, and H.E. Stanley, *Nature*, **418**, 955 (2002); *ibid*, **421**, 764 (2003).
12. S. Roche and E. Macia, *Mod. Phys. Lett. B*, **18**, 847 (2004).
13. V.M. Apalkov and T. Chakraborty, *Phys. Rev. B*, **71**, 33102 (2005).
14. V. Apalkov, X.F. Wang, and T. Chakraborty, in *Charge Migration in DNA: Perspectives from Physics, Chemistry, and Biology* edited by T. Chakraborty (Springer, 2007).
15. H. Sugiyama and I. Saito, *J. Am. Chem. Soc*., **118**, 7063 (1996); H.Y. Zhang, X.Q. Li, P. Han, X.Y. Yu and Y.J. Yan, *J. Chem. Phys*., **117**, 4578 (2002).
16. W. Ren, J. Wang, Z.S. Ma and H. Guo, *Phys. Rev. B*, **72**, 035456 (2005).
17. S.D. Wetmore, R.J. Boyd and L.A. Eriksson, *Chem. Phys. Lett*., **322**, 129 (2000).
18. A.A. Voityuk, J. Jortner, M. Bixon and N. Rösch, *J. Chem. Phys*., **104**, 9740 (2000); *ibid*., **114**, 5614 (2001); A. Troisi and G. Orlandi, *Chem. Phys. Lett*., **344**, 509 (2001).
19. H. Basch, R. Cohen and M.A. Ratner, *Nano Lett*., **5**, 1668 (2005); F. Zahid, M. Paulsson, E. Polizzi, A.W. Ghosh, L. Siddiqui and S. Datta, *J. Chem. Phys*., **123**, 064707 (2005).
20. G.C. Liang, A.W. Ghosh, M. Paulsson and S. Datta, *Phys. Rev. B*, **69**, 115302 (2004).
21. M. Singh, C. S. Wang, and J. Callaway, *Phys. Rev. B*, **11**, 287 (1975).
22. D.L. Rogers, *Phys. Stat. Sol. (B)*, **66**, K53 (1974).